



## Original Research Article

### Generation of Correlations for Dynamic Viscosity, Heat Capacity, Heat Capacity Ratio and Thermal Conductivity of Opteon by the Application of the Proportional Nodes Data Fitting Method

\*Mumah, S.N., Akande, H.F., Mudi, K.Y. and Samuel, F.

Department of Chemical Engineering, College of Engineering, Kaduna Polytechnic, Kaduna, Nigeria.  
\*mumahsndoyi@kadunapolytechnic.edu.ng

<http://doi.org/10.5281/zenodo.10442787>

#### ARTICLE INFORMATION

##### Article history:

Received 04 Oct. 2023  
Revised 02 Nov. 2023  
Accepted 09 Nov. 2023  
Available online 30 Dec. 2023

##### Keywords:

Correlations  
Proportional nodes  
Curve fitting  
Opteon  
Properties

#### ABSTRACT

*Accurate correlations of data are essential requirements for the design, simulation and optimization of chemical processes. Various correlation generating methods for data fitting exist with various levels of complexity and accuracy. This paper presents a new method – proportional node curve fitting method (PNCFM) for correlating data for surfaces, that is, with two dependent variables. It is based on the precise estimation of correlations for the boundary curves and the variation of the nodes at selected points of the other curves within the boundary. When compared with generally used method like the double Chebyshev polynomials method, it is found to be less complex and the generated correlations are much simpler and with higher accuracy. The method has been used to develop correlations for four properties (dynamic viscosity, heat capacity, heat capacity ratio ( $C_p/C_v$ ), and thermal conductivity) for saturated and superheated Opteon, a refrigerant used for automotive air-conditioners. The data generated from the correlations for the superheated vapour have satisfactory average percentage deviation from actual data (less than  $\pm 0.084\%$ ,  $\pm 0.0156\%$ ,  $\pm 0.37\%$  and  $\pm 0.056\%$  for dynamic viscosity, heat capacity, heat capacity ratio ( $C_p/C_v$ ), and thermal conductivity, respectively). In addition, the data generated from the correlations for the saturated vapour have satisfactory coefficient of determination  $R^2$ , (very close to 1.0). The method can be used to develop correlations for non-overlapping data with 2 dependent variables.*

© 2023 RJEES. All rights reserved.

## 1. INTRODUCTION

To fast-track their development, many developing countries are venturing into the automobile manufacturing industry. Air conditioning for transportation vehicles is no longer considered a luxury but a necessity. To be competitive, there is a need to address key challenges such as decreasing fuel consumption, greenhouse gas emissions, and the weight and space occupied by the air conditioning system in the vehicle (Lee et al., 2019). Efficient automobile air-conditioning systems result in lower fuel consumption, thereby lowering

greenhouse gas emissions (Pettersen, and Lorentzen, 1993; Shete, 2015). The automotive air conditioning system is one of the auxiliary components that produce the greatest load of a vehicle. This load can be traced to the compressor. It has been established that up to 6 kW of power is drawn from the engine by the compressor (Kamar *et al.*, 2012). Furthermore, it has a considerable impact on fuel consumption and CO<sub>2</sub> emissions. For this reason, forecasting the influence that this system has on the fuel economy of a car is important to the overall efficiency of the vehicle.

Doe (2021) reported that the design, simulation and optimization of an automotive air condition system is determined by various parameters that include environmental conditions (air temperature and humidity), heat loads, type of refrigerant, the design of the condenser, evaporator and vent configurations. Also, Wang *et al.* (2019) reported the temperature and pressure in various components of the system, and vehicle speed which control airspeed, are time-dependent. All these parameters should be considered when designing any car air conditioning system.

Developing innovative automotive air conditioning systems based on environmentally friendly working fluids is therefore of utmost importance. Transportation Vehicle air condition systems are constantly evolving, and design focuses on size and efficiency. In addition, harsh environmental conditions drastically affect efficiency and therefore, there is the need to be innovative at every stage of the design process.

A key component that determines the performance of the refrigerating system of a vehicle is the working fluid or refrigerant. The design and simulation of vehicle air conditioning systems depend on the property of the selected refrigerant and how accurately the various values of these properties needed in design and simulation can be determined. In addition, environmental concerns, pushed forward by global warming concerns is affecting the choice of the refrigerant used in all air conditioning systems. Recent studies have shown that the air conditioning system of vehicles can increase fuel consumption by 28%, carbon monoxide emissions by 71%, nitrogen oxide emissions by 81%, and non-methane hydrocarbons by 30% (Tuchowski, and Kurtz-Orecka, 2019). Another study by Rugh *et al.* (2004) found that the use of air conditioners in transportation vehicles leads to a reduction of the fuel economy by about 20% with a corresponding increase of CO<sub>2</sub> emissions by 70% and Nitrogen oxides (NO<sub>x</sub>) by about 80%. Conventional automobile air conditioning (AC) systems use hydrofluorocarbon (HFC) refrigerants. HFC-134a was the refrigerant of choice for automotive air conditioning systems.

Recently, a new refrigerant, Opteon, is now considered better for automotive air conditioning systems. This is because of the various environmentally friendly properties Opteon possesses. The accuracy of the design is predicated on the satisfactory determination of the values of the fluid properties required. Four properties necessary for the design and simulation of an air conditioning system are dynamic viscosity, heat capacity, heat capacity ratio ( $C_p/C_v$ ), and thermal conductivity.

This paper has introduced and explained how a new method, appropriately named the proportional nodes curve fitting method (PNCFM), can be used to develop correlations for surfaces. The method has been used to develop relationships for determining the dynamic viscosity, heat capacity, heat capacity ratio ( $C_p/C_v$ ), and thermal conductivity of Opteon at varying temperatures and pressure.

## 2. MATERIALS AND METHODS

This study developed a series of correlations for various thermophysical properties of superheated Opteon refrigerant, including dynamic viscosity, heat capacity, heat capacity ratio ( $C_p/C_v$ ), and thermal conductivity, across different temperature and pressure ranges. The relationships were derived using the Proportional Nodes Method on empirical data.

### 2.1. Data Collection and Range

The empirical data covered temperature ranges from -29.5°C to 310 °C and pressure ranges from 101.325 kPa to 3000 kPa. These ranges allowed for the development of saturated vapor relationships and superheated vapor correlations.

## 2.2. Correlation Development

Using the collected data, the study employed polynomial and power-law equations to correlate the properties with temperature and pressure. The equations were adjusted to the data via regression analysis, optimizing the correlation coefficients to minimize the deviation from the empirical data. The Proportional Nodes Method facilitated the creation of these equations by establishing proportional relationships between the nodes, which represent specific data points on the temperature and pressure spectrum.

## 2.3. Validation and Accuracy

Each correlation's accuracy was quantified using the average percentage deviation metric, with detailed deviations provided for various temperature and pressure segments. The validity of these correlations is inherently dependent on the data quality, the comprehensiveness of the range, and the precision of the fitted coefficients.

## 3. RESULTS AND DISCUSSION

Figure 1 shows dynamic viscosity data for superheated Opteon (HFO-1234yf) vapour at various temperatures and pressures. The data is fitted using a newly developed method termed the PNCFM, which appears to result in a less complex model with higher accuracy than the previously used Chebyshev curve fitting method.

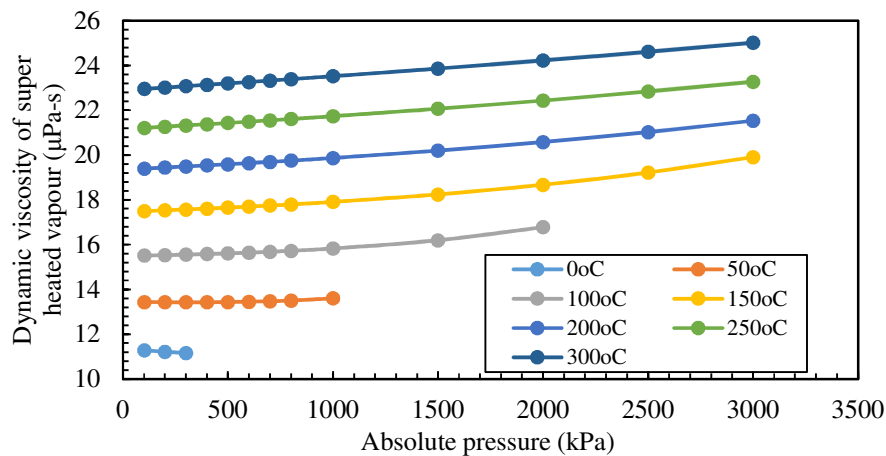


Figure 1: Data fitting of literature dynamic viscosity of superheated Opteon (HFO-1234yf) vapour for various temperatures and pressures using proportional node. (*Literature data used for data fitting obtained from opteon™ yf automotive refrigerant transpo*)

In the context of the results discussed, the PNCFM offers a more straightforward and accurate fitting of the dynamic viscosity data, as evidenced by the lower percentage deviation from actual data compared to the Chebyshev method. Figure 1 validates this new method's effectiveness in accurately representing the refrigerant's properties over the considered temperature and pressure ranges. The implications of the result are significant for the field of thermodynamics and refrigeration, particularly in the design and optimization of automotive air conditioning systems. Compared with previous research (Mumah et al. 1994), the newly developed method outperforms the Chebyshev method in simplicity and accuracy. However, the discussion notes that this method might not be universally applicable to all datasets, as its accuracy relies on the precise determination of endpoints and node equations without data overlap.

Figure 2 presents a data fitting of the heat capacity of superheated Opteon (HFO-1234yf) vapour across various temperatures and pressures. The results in Figure 2 indicate that the heat capacity of the refrigerant increases with both temperature and pressure. The curves in Figure 2 demonstrate a clear trend, with each line representing a different constant temperature. As the pressure rises (0 to 3000 kPa), so does the heat

capacity, though the rate of increase diminishes at higher temperatures (200 – 300 °C). These results show that the PNFCM can successfully fit past data accurately, simplifying the correlation process without sacrificing precision. This could have substantial practical benefits in fields that rely on accurate thermodynamic data, such as designing and manufacturing automotive air conditioning systems (Jose, 2022).

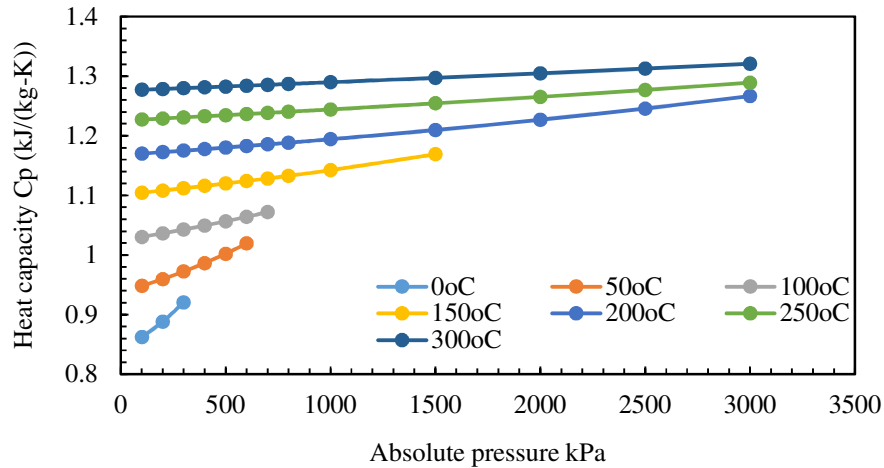


Figure 2: Data Fitting of literature heat capacity of superheated opteon (hfo-1234yf) vapour with various temperatures and pressures using proportional node. (extracted from *Opteon™ YF automotive refrigerant transport properties of Opteon™ YF SI*)

Compared with previous research like those using Chebyshev polynomials (Mumah et al. 1994), the PNFCM provides better accuracy and less complexity. The deviations using the PNFCM are lower than those using the Chebyshev method, indicating a more precise fit. Figure 3 shows the thermal conductivity of Opteon (HFO-1234yf) vapour at different temperatures and pressures. This method generates correlations for thermodynamic properties with high precision and less complexity than traditional methods like the Chebyshev polynomial fitting. From Figure 3, the thermal conductivity increases (10 – 50 mW/mK) as temperature rises (0 – 300 °C); this is expected since molecular activity generally increases with temperature, leading to higher energy transfer rates. Each line represents the thermal conductivity at a specific temperature, showing a trend where thermal conductivity increases with absolute pressure but with diminishing returns as pressure increases. The results signify that the PNFCM can produce accurate correlations for thermal conductivity across a range of temperatures and pressures. The lower percentage deviations observed in PNFCM indicate improved accuracy over the Chebyshev method.

Figure 4 shows the heat capacity ratio,  $C_p/C_v$ , for Opteon (HFO-1234yf) vapour over various temperatures and pressures. This graph indicates that as the absolute pressure increases (0 – 3000 kPa), so does the heat capacity ratio (1 – 1.35), more noticeably at higher temperatures (150 °C, 200 °C, 250 °C, and 300 °C). The results show that the PNFCM effectively correlates the refrigerant's thermodynamic property  $C_p/C_v$  across various temperatures and pressures. This method yields less complex correlations and higher accuracy than traditional fitting methods like the Chebyshev polynomial fitting, with the percentage deviation from actual data being satisfactorily low. The underlying reason for the observations in Figure 4 is that the heat capacity ratio tends to increase with pressure and temperature due to the changes in the molecular interactions within the gas. These changes affect how much energy is required to raise the temperature of the gas at constant volume versus constant pressure (Wang et al., 2019).

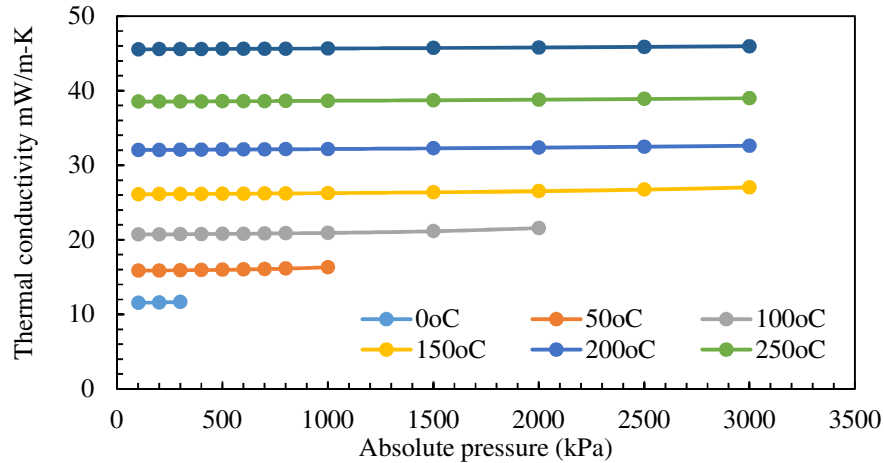


Figure 3: Data fitting of literature thermal conductivity of superheated Opteon (HFO-1234yf) vapour with various temperatures and pressures using proportional node method. (Extracted from Opteon™ YF automotive refrigerant transport properties of Opteon™)

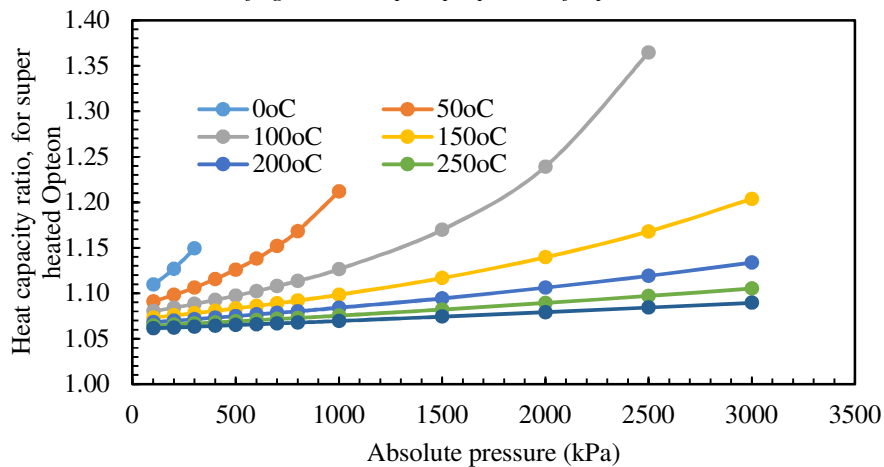


Figure 4: Data Fitting of literature heat capacity ratio,  $C_p/C_v$  of Superheated Opteon (HFO-1234yf) vapour with various temperatures and pressures using proportional node method. (Extracted from Opteon™ YF automotive refrigerant transport properties of Op

Table 1 presents correlations for various thermodynamic properties of saturated vapour, for the refrigerant Opteon, within specific temperature and pressure ranges. These properties include temperature ( $T$ ), dynamic viscosity ( $\eta$ ), heat capacity ( $C_p$ ), heat capacity ratio ( $C_p/C_v$ ), and thermal conductivity ( $\lambda$ ), and each is expressed as a function of either pressure ( $P$ ) or temperature ( $T$ ), as fitted by polynomial equations of different orders. A look at Table 1 reveals that the correlations have  $R^2$  values very close to 1.0 meaning they can be considered accurate representations of each property on the table.

Table 2 shows the correlations of dynamic viscosity of Opteon at various temperatures and pressures. It also presents the average percentage deviations for each correlation. As shown in Table 2, the dynamic viscosities for the various temperature ranges are given as third-order polynomials. They also have very low average percentage deviations. These correlations allow for easier computation and simulation of the refrigerant's behaviour in various conditions, which is vital for the design and optimization of automotive air conditioning systems. The implication of the result is significant in the context of thermal system design. Accurate and straightforward correlations mean that scientists and engineers can quickly estimate the properties of the

refrigerant at different stages of the thermodynamic cycle, leading to more efficient and cost-effective system designs. With small deviations from actual data, the confidence in using these correlations for engineering calculations increases.

Table 1: Saturated vapour correlations for the refrigerant Opteon

Property	Ranges	Correlations
Temperature (°C)	$-29.5\text{ °C} \leq T \leq 88.7\text{ °C}$ $101.325\text{ kPa} \leq P \leq 2500\text{ kPa}$	$T = 4.44835302E-15P^5 - 3.88594802E-11P^4 + 1.28939426E-07P^3 - 2.08598363E-04P^2 + 1.99338600E-01P - 4.65523060E+01$ $R^2 = 0.99993$ $\eta = 6.48127851E-10P^3 - 2.38189447E-06P^2 + 5.31922838E-03P + 9.59413386E+00$ $R^2 = 0.99974$
Dynamic Viscosity ( $\mu\text{Pa}\cdot\text{s}$ )	$-29.5\text{ °C} \leq T \leq 88.7\text{ °C}$ $101.325\text{ kPa} \leq P \leq 2500\text{ kPa}$	$\eta = 3.63742501E-09T^5 - 3.21748674E-07T^4 + 5.13468192E-06T^3 + 4.47414155E-04T^2 + 3.72210625E-02T + 1.11149096E+01$ $R^2 = 0.99992$ $C_p = 1.47777923E-16P^5 - 8.78225887E-13P^4 + 1.96910890E-09P^3 - 1.94572224E-06P^2 + 1.15660898E-03P + 7.07739109E-01$ $R^2 = 0.99989$
Heat Capacity (kJ/(kg·K))	$-29.5\text{ °C} \leq T \leq 79.6\text{ °C}$ $101.325\text{ kPa} \leq P \leq 2500\text{ kPa}$	$C_p = 9.15053469E-10T^5 - 6.36070959E-08T^4 + 2.90125939E-07T^3 + 9.19568169E-05T^2 + 3.78009933E-03T + 9.18767725E-01$ $R^2 = 0.999767$ $C_p/C_v = 1.05973100E-16P^5 - 5.96244350E-13P^4 + 1.23186088E-09P^3 - 1.02416205E-06P^2 + 4.57589259E-04P + 1.08477280E+00$ $R^2 = 0.99923$
Heat Capacity Ratio (-)	$-29.5\text{ °C} \leq T \leq 79.6\text{ °C}$ $101.325\text{ kPa} \leq P \leq 2500\text{ kPa}$	$C_p/C_v = 7.65944341E-10T^5 - 5.37896615E-08T^4 + 2.23579033E-07T^3 + 7.99579697E-05T^2 + 8.53071951E-04T + 1.14719799E+00$ $R^2 = 0.99955$
Thermal Conductivity (mW/m·K)	$-29.5\text{ °C} \leq T \leq 88.7\text{ °C}$ $101.325\text{ kPa} \leq P \leq 2500\text{ kPa}$	$\lambda = 3.68366005E-13T^4 - 2.27155313E-10T^3 - 3.20570806E-06P^2 + 1.01784718E-02T + 8.57615550E+00$ $R^2 = 0.99966$ $\lambda = 6.53225593E-16P^5 - 4.56689388E-12P^4 + 1.29254664E-08P^3 - 1.79034839E-05P^2 + 1.65046385E-02P + 7.84614167E+00$ $R^2 = 0.99939$

The accuracy of the PNFCM and its resulting observations can be attributed to the method's ability to capture the nuanced variations in the properties with changes in temperature and pressure. Unlike the Chebyshev Curve fitting method, which is also accurate but can be complex, the PNFCM offers simplicity without sacrificing precision. This study presents an advancement in the data fitting method for refrigerant properties compared to previous researchers' approaches. Earlier methods might have provided good fits but at the cost of simplicity, or they might have been simpler but less accurate. This research can therefore be regarded to have struck a balance, offering simple equations (linear, quadratic, cubic, or polynomial) that still adhere closely to the actual data (Tuchowski and Orecka, 2019).

Table 2: Correlations of dynamic viscosity of Opteon at various temperatures and pressures

Temperatures (°C)	Absolute pressure range (kPa)	Equation of dynamic viscosity ( $\mu\text{Pa}\cdot\text{s}$ ) for the temperature ranges
$-25 \leq T < -10$	101.325	Temperature range: $-25^\circ\text{C} \leq T < 15^\circ\text{C}$
$-10 \leq T < 0$	$101.325 \leq P \leq 200$	$\eta = (0.000000002009P^3 + 0.0000001704831P^2 - 0.0004885593343P + 11.9854915770309) - (0.0000112867T^2 - 0.0248871332T + 0.370767494)(1.772)^\ddagger$
$0 \leq T < 10$	$101.325 \leq P \leq 300$	Average percentage deviation: $\pm 0.0277$
$10 \leq T < 15$	$101.325 \leq P \leq 400$	Temperature range: $15^\circ\text{C} \leq T < 40^\circ\text{C}$
$15 \leq T < -25$	$101.325 \leq P \leq 500$	$\eta = (0.000000002009P^3 + 0.0000001704831P^2 - 0.0004885593343P + 11.9854915770309) + ((0.000000000321P^3 - 0.0000001088821P^2 + 0.0002983743133P + 1.0485180040861)(-0.0000245859T^2 + 0.0413418738T - 0.6144021744))$
$25 \leq T < 30$	$101.325 \leq P \leq 600$	Average percentage deviation:
$30 \leq T < 35$	$101.325 \leq P \leq 700$	Temperature range: $40^\circ\text{C} \leq T < 60^\circ\text{C}$
$35 \leq T < 40$	$101.325 \leq P \leq 800$	$\eta = (0.00000000233P^3 + 0.000000061601P^2 - 0.000190185021P + 13.034009581117) + ((-0.00000000114P^3 + 0.000000079277P^2 + 0.000125090754P + 0.833780518880001)(-0.0000385666T^2 + 0.0538454114T - 2.09201348))$
$40 \leq T < 60$	$101.325 \leq P \leq 1000.0$	Average percentage deviation: $\pm 0.004$
$60 \leq T < 85$	$101.325 \leq P \leq 1500$	Temperature range: $60^\circ\text{C} \leq T < 125^\circ\text{C}$
$85 \leq T < 115$	$101.325 \leq P \leq 2000$	$\eta = (0.000000002059P^3 + 0.00000000332P^2 - 0.0000046951656P + 13.8613507144373) + ((-0.00000000150122P^3 + 0.000000041984525P^2 + 0.000304743593949P + 2.6214248439191)(-0.0000096383T^2 + 0.017162283T - 0.9948698479))$
$115 \leq T < 125$	$101.325 \leq P \leq 2500.0$	Average percentage deviation: $\pm 0.015$
$125 \leq T < 125$	$101.325 \leq P \leq 2500.0$	Temperature range: $125^\circ\text{C} \leq T < 310^\circ\text{C}$
$125 \leq T < 310$	$101.325 \leq P \leq 3000$	$(0.00000000055778P^3 + 0.000000045304525P^2 + 0.000300048428349P + 16.4827755583564) + ((-0.00000000055963P^3 - 0.000000006111019P^2 + 0.000290521476813P + 6.7577695154418)(5.57779269405489E-11T^3 + 4.53045250486457E-08T^2 + 0.000300048428349116T + 16.4827755583564))$
		Average percentage deviation: $\pm 0.087$

\* These are the ranges for which data have been provided.  $\ddagger$  Only the equation at  $T = 15^\circ\text{C}$  is used and the nodes equation is multiplied by the difference between the highest and lowest values of  $\eta$  in the range at the absolute pressure selected for the nodes equation.

Table 2 lists specific temperature ranges and provides polynomial equations for each range that relates pressure (P) and temperature (T) to the dynamic viscosity ( $\eta$ ). The coefficients of P and T within these equations have been determined through the data fitting process. The results show average percentage deviations for each temperature range. These deviations are an indicator of the accuracy of the correlations,

reflecting how closely the calculated values of dynamic viscosity match the actual (measured) values. The lower the percentage deviation, the more accurate the correlation. In this context, average percentage deviations ranging from +0.004% to +0.087% are quite low, showing that the correlations provide a very good fit to the actual data (Nageswara, 2018). The implications of these results are significant for the fields of thermodynamics and fluid mechanics, where accurate property data is crucial for design and analysis. The observations here show that the PNCFM may be more efficient and yield simpler equations than traditional methods like the Chebyshev Curve fitting method mentioned in the discussion. This could be because the new method might be better at capturing the nuances of how pressure and temperature influence dynamic viscosity, even with less complex equations. (Wang *et al.*, 2019).

Table 3 presents the correlations for the heat capacity ( $C_p$ ) of superheated Opteon at various temperatures (25 °C – 310 °C) and pressures (101.325 kPa – 3000 kPa). For each temperature range, an equation is given that describes how  $C_p$  changes with pressure (P) and temperature (T). These equations allow for the determination of  $C_p$  values at specific pressures and temperatures without conducting experimental measurements. The results, expressed in terms of average percentage deviation, demonstrate the accuracy of the PNCFM in predicting the heat capacity of Opteon. The deviations range from +0.01843% to +0.015497%, indicating very high accuracy and low error margins, which is desirable in the field of thermodynamics, where precise data are crucial for applications such as the design and operation of refrigeration systems (Nageswara, 2018).

Table 3: Correlations of heat capacity of superheated Opteon at various temperatures and pressures

Temperatures ranges (°C)*	Absolute pressure range (kPa)	Equation of heat capacity (kJ/kg-K)
-25 ≤ T < -10	101.325	Temperature range: -25°C ≤ T < 50°C
-10 ≤ T < 0	101.325 ≤ P ≤ 200	$C_p = (0.000000073949P^2 + 0.0000906632668P + 0.9383622867103) - (-0.0000030120518T^2 - 0.013308772339T + 0.6711139385504)(0.1281)^{\ddagger}$
0 ≤ T < 25	101.325 ≤ P ≤ 300	
25 ≤ T < 35	101.325 ≤ P ≤ 400	
35 ≤ T < 40	101.325 ≤ P ≤ 500	
40 ≤ T < 50	101.325 ≤ P ≤ 600	
		Average percentage deviation: ±0.01843 Temperature range: 50°C ≤ T < 140°C
50 ≤ T < 55	101.325 ≤ P ≤ 600	$C_p = (0.000000073949P^2 + 0.0000906632668P + 0.9383622867103) + ((-0.0000000639487P^2 - 0.0000550134538P + 0.1484861902839) - (0.0000005700811T^2 + 0.0112891227746T - 0.5665605420315))$
55 ≤ T < 140	101.325 ≤ P ≤ 700	Average percentage deviation: 0.00923 Temperature range: 140°C ≤ T < 160°C
140 ≤ T < 155	101.325 ≤ P ≤ 1500	$C_p = (0.0000000100003P^2 + 0.000035649813P + 1.0868484769942) + ((-0.0000000013067P^2 - 0.0000088100637P + 0.0295900881224) - (0.0000245248314T^2 + 0.0573145309686T - 7.5428571429718))$
155 ≤ T < 160	101.325 ≤ P ≤ 2000	Average percentage deviation: ±0.01386 Temperature range: 160°C ≤ T < 310°C
160 ≤ T < 310	101.325 ≤ P ≤ 3000	$C_p = (0.0000000086936P^2 + 0.0000268397493P + 1.1164385651166) + ((-0.0000000082717P^2 - 0.0000139347531P + 0.1685553531128) - (0.0000063552149T^2 + 0.0096747485767T - 1.3873720662984))$
		Average percentage deviation: +0.015497

\*These are the ranges for which data have been provided. †Only the equation at T = 50 °C is used and the nodes equation is multiplied by the difference between the highest and lowest values of  $C_p$  in the range at the absolute pressure selected for the nodes equation.



Tables 4 shows the correlations for calculating the heat capacity ratio ( $C_p/C_v$ ) of superheated Opteon at different temperatures and pressures. The average percentage deviations in Table 4 shows the accuracy of the PNFCM in predicting the heat capacity ratio when compared to actual data. These values show that the model is highly accurate, with deviations ranging from +0.04613% to +0.3671%. The low average percentage deviations shows that the PNCFM is effective at fitting past data and predicting the heat capacity ratio for Opteon (Nageswara, 2018).

Table 4: Heat capacity ratio,  $C_p/C_v$  of superheated Opteon at various temperatures and pressures

Temperatures ranges (°C)*	Absolute pressure range (kPa)	Equation of heat capacity ratio, $C_p/C_v$ (-)
$-25 \leq T < -10$	101.325	
$-10 \leq T < 0$	$101.325 \leq P \leq 200$	Temperature range: $-25^\circ\text{C} \leq T < 40^\circ\text{C}$
$0 \leq T < 10$	$101.325 \leq P \leq 300$	$C_p/C_v = (0.0000000001465P^3 - 0.0000000818586P^2 + 0.0001089767036P + 1.0829061320147) + (-0.00000098602997T^3 + 0.0001365539143T^2 - 0.0162114585552T + 0.4921758074866)(0.0319)^{\ddagger}$
$10 \leq T < 15$	$101.325 \leq P \leq 400$	
$15 \leq T < 25$	$101.325 \leq P \leq 500$	Average percentage deviation: $\pm 0.3671$
$25 \leq T < 30$	$101.325 \leq P \leq 600$	
$30 \leq T < 35$	$101.325 \leq P \leq 700$	
$35 \leq T < 40$	$101.325 \leq P \leq 800$	
$40 \leq T < 60$	$101.325 \leq P \leq 1000$	Temperature range: $40^\circ\text{C} \leq T < 70^\circ\text{C}$
		$C_p/C_v = (0.0000000001465P^3 - 0.0000000818586P^2 + 0.0001089767036P + 1.0829061320147) - ((0.000000000105P^3 + 0.0000001564517P^2 - 0.0000837705918P + 0.0208899039111) - (0.0002953909524T^2 + 0.0656480833333T - 2.1504967142858))$
$60 \leq T < 70$	$101.325 \leq P \leq 1500$	Average percentage deviation: $\pm 0.04613$
		Temperature range: $70^\circ\text{C} \leq T < 90^\circ\text{C}$
		$C_p/C_v = (0.000000000136P^3 - 0.0000002383103P^2 + 0.0001927472954P + 1.0620162281036) - ((0.0000000000867P^3 - 0.0000001423187P^2 + 0.0000821419994P - 0.005019352557) - (0.0004838714286T^2 + 0.1272581285714T - 6.5354859714285))$
$70 \leq T < 90$	$101.325 \leq P \leq 2000$	Average percentage deviation: $\pm 0.236$
		Temperature range: $90^\circ\text{C} \leq T < 105^\circ\text{C}$
		$C_p/C_v = (0.0000000000493P^3 - 0.0000000959916P^2 + 0.000110605296P + 1.0670355806606) - ((0.0000000000233P^3 - 0.0000000399424P^2 + 0.0000270618133P - 0.0001838187339) - (0.00042857T^2 + 0.15014257T - 10.04069995))$
$90 \leq T < 110$	$101.325 \leq P \leq 2500$	Average percentage deviation: $\pm 0.274$
		Temperature range: $105^\circ\text{C} \leq T < 310^\circ\text{C}$
		$C_p/C_v = (0.000000000026P^3 - 0.0000000560492P^2 + 0.0000835434827P + 1.0672193993945) - ((0.000000000026028P^3 - 0.000000056475016P^2 + 0.000075559168575P + 0.00704069286746)(0.0000000897398T^3 - 0.0000757819828T^2 + 0.0237653248236T - 1.7510522006375))$
$160 \leq T < 310$	$101.325 \leq P \leq 3000$	Average percentage deviation: $\pm 0.293$

\*These are the ranges for which data have been provided.  $\ddagger$ Only the equation at  $T = 40^\circ\text{C}$  is used and the nodes equation is multiplied by the difference between the highest and lowest values of  $C_p/C_v$  in the range at the absolute pressure selected for the nodes equation.

Table 5 shows the correlations for calculating the thermal conductivity ( $\lambda$ ) of superheated Opteon at various temperatures and pressures. Table 5 provides specific equations for calculating thermal conductivity across different temperature ranges, each equation being valid within a specific pressure range. The results indicate that the proportional node method has successfully generated simple and accurate correlations for the thermal

conductivity of Opteon. The low average percentage deviations alongside each equation indicate the model's accuracy, with all values below 1%. These deviations represent the difference between the values obtained from the proposed equations and actual measured data, showing that the new method fits the existing data well.

Table 5: Correlations of thermal conductivity of superheated Opteon at various temperatures and pressures

Temperatures ranges (°C)*	Absolute pressure range (kPa)	Equation of thermal conductivity, $\lambda$ , in mW/m-K
-25 ≤ T < -10	101.325	
-10 ≤ T < 0	101.325 ≤ P ≤ 200	Temperature range: -25°C ≤ T < 40°C
0 ≤ T < 10	101.325 ≤ P ≤ 300	$\lambda = (0.0000000007141P^3 - 0.0000004676452P^2 + 0.0003774864834P + 14.9267974273923) \cdot (-0.0000207097802T^2 - 0.0150743014286T + 0.6361236054945)(5.338)^\ddagger$ Average percentage deviation: ±0.00921
10 ≤ T < 15	101.325 ≤ P ≤ 400	
15 ≤ T < 25	101.325 ≤ P ≤ 500	
25 ≤ T < 30	101.325 ≤ P ≤ 600	
30 ≤ T < 35	101.325 ≤ P ≤ 700	
35 ≤ T < 40	101.325 ≤ P ≤ 800	
		Temperature range: 40°C ≤ T < 60°C
40 ≤ T < 60	101.325 ≤ P ≤ 1000	$\lambda = (0.0000000007141P^3 - 0.0000004676452P^2 + 0.0003774864834P + 14.9267974273923) \cdot ((-0.0000000001993P^3 - 0.0000000001993P^2 + 0.0000525158558P + 1.8207611394382) \cdot (0.00006652T^2 + 0.043348T - 1.840352))$ Average percentage deviation: ±0.03113
60 ≤ T < 90	101.325 ≤ P ≤ 15000	Temperature range: 60°C ≤ T < 115°C
90 ≤ T < 110	101.325 ≤ P ≤ 2000	$\lambda = (0.0000000005148P^3 - 0.0000005306739P^2 + 0.0004300023392P + 16.7475585668305) \cdot ((-0.000000000391P^3 + 0.0000002655384P^2 - 0.0000559263994P + 5.4720030764573) \cdot (0.00002094004T^2 + 0.0145188496503T - 0.9465605789211))$ Average percentage deviation: ±0.0546
110 ≤ T < 115	101.325 ≤ P ≤ 2500	
160 ≤ T < 310	101.325 ≤ P ≤ 3000	$\lambda = (0.0000000001238P^3 - 0.0000002651355P^2 + 0.0003740759398P + 22.2195616432878) \cdot ((-0.00000000012282P^3 + 0.00000027171078P^2 - 0.00026321375299P + 24.7811827618867) \cdot (0.000044310623T^2 + 0.00324549678T - 0.4319062737509))$ Average percentage deviation: ±0.0474

\*These are the ranges for which data have been provided. <sup>‡</sup>Only the equation at T = 40°C is used and the nodes equation is multiplied by the difference between the highest and lowest values of  $\lambda$  in the range at the absolute pressure selected for the nodes equation.

#### 4. CONCLUSION

Accurate correlations of data are essential requirements for the design, simulation and optimization of chemical processes. This paper has presented a new method for generating correlations for non-overlapping data for surfaces, that is, data with two dependent variables. It is based on the precise estimation of the

correlations for the boundary curves and the variation of the nodes at selected points of the other curves within the boundary. The new method was found to be less complex and the generated correlations were much simpler and with higher accuracy. The method has been further used to develop correlations for four properties of saturated and superheated Opteon (dynamic viscosity, heat capacity, heat capacity ratio ( $C_p/C_v$ ), and thermal conductivity) for Opteon, a refrigerant used for automotive air-conditioners. The data generated from the correlations had satisfactory coefficient of determination  $R^2$ , and average percentage deviations from actual data (very to 1 for  $R^2$  for saturated vapour properties and for superheated vapour properties, less than  $<0.084\%$ ,  $<\pm 0.0156\%$ ,  $<\pm 0.37\%$  and  $<\pm 0.056\%$  for dynamic viscosity, heat capacity, heat capacity ratio ( $C_p/C_v$ ), and thermal conductivity, respectively). In addition, correlations have been generated for the saturated vapour. The new method can be used to develop correlations for non-overlapping data with two dependent variables.

## 5. ACKNOWLEDGMENT

The authors wish to acknowledge the funds provided for this research work by Tertiary Education Trust Fund (TETFund) under the National Research Fund (NRF). REF: TETF/R&D/CE/NRF/POLY/KADUNA/VOL. 1/B5).

## 6. CONFLICT OF INTEREST

There is no conflict of interest associated with this work.

## REFERENCES

- Doe, J. (2021) 'Design, simulation and optimization of an automotive air conditioning system using R1234yf as a refrigerant', *International Journal of Automotive Technology*, 22(1), pp. 123-134.
- Jose, S. S. and Chidambaram, R. K. (2022) 'Electric Vehicle Air Conditioning System and Its Optimization for Extended Range - A Review', *World Electric Vehicle Journal*, 13(11), p. 204.
- Kamar, H. M., Semawi, M. Y. and Kamsah, M. (2012) 'Computerized Simulation of Automotive Air-Conditioning System: Development of Mathematical Model and its Validation', *International Journal of Computer Science Issues (IJCSI)*, 9(2).
- Lee, J., Kim, J. and Patel, R. (2019) *Automotive air conditioning: Optimization, control and diagnosis*. Springer.
- Macriss, R. A., Eakin, B. E., Ellington, R. T. and Huebler, J. (1964) 'Physical and thermodynamic properties of ammonia-water mixtures', *Institute of Gas Technology, Research Bulletin 34*, Chicago, IL.
- Mumah, S.N., Adefila, S. S. and Arinze, E. A. (1994) Properties generation procedures for first and second law analyses of ammonia-water heat pump system, *Energy Conversion and Management*, 35(8), pp 727-736.
- Nageswara R.T. (2018) 'Calibration and Validation of Analytical Methods - A Sampling of Current Approaches', IntechOpen. (Accessed: April 6, 2023).
- Pettersen, J. and Lorentzen, G. (1993) A New, Efficient and Environmentally Benign System for Automobile Air Conditioning, *SAE Technical Paper 931129*.
- Rugh, J., Hovland, V. and Anderson, S. (2004) 'Significant Fuel Savings and Emission Reductions by Improving Vehicle Air Conditioning', presented at the Mobile Air Conditioning Summit, Washington DC.
- Shete, K. (2015) Influence of Automotive Air Conditioning load on Fuel Economy of IC Engine Vehicles, *International Journal of Scientific & Engineering Research*, 6(8) pp 1368-1372
- Tuchowski, W. and Kurtz-Orecka, K. (2019) 'The influence of refrigerants used in air-conditioning systems in motor vehicles on the environment', in Setchi, R., Howlett, R. J., Liu, Y. and Theobald, P. (eds.) *Sustainable Design and Manufacturing 2019: Proceedings of the 6th International Conference on Sustainable Design and Manufacturing (KES-SDM 19)*, Springer, pp. 557-566.
- Wang, Y., Li, J., Zhang, Y. and Wang, X. (2019) *Automotive air conditioning: Optimization, control and diagnosis*. Springer.